

A Novel Mapping and Navigation Framework for Robot Autonomy in Orchards

Yaoqiang Pan¹, Hao Cao¹, Kewei Hu¹, Hanwen Kang^{1,*}, Xing Wang^{2,*}

¹ College of Engineering, South China Agriculture University, China

² Robotics and Autonomous System, Data 61, CSIRO, Australia

* Correspondence Author

Resumen—Target detection is a basic task to divide the object types in the orchard point cloud global map, which is used to count the overall situation of the orchard. And provide necessary information for unmanned navigation planning of agricultural vehicles. In order to divide the fruit trees and the ground in the point cloud global map of the standardized orchard, and provide the orchard overall information for the path planning of autonomous vehicles in the natural orchard environment. A fruit tree detection method based on the Yolo-V7 network is proposed, which can effectively detect fruit tree targets from multi-sensor fused radar point cloud, reduce the 3D point cloud information of the point cloud map to 2D for the fruit tree point cloud in the Yolo-V7 network detection map, and project the prediction results into the point cloud map. Generally, the target detection network based on PointNet has the problem of low speed and large computational load. The method proposed in this paper is fast and low computational load and is suitable for deployment in mobile robots. From the experimental results, the recall rate and accuracy rate of the proposed method in orchard fruit tree detection are 0.4 and 0.696 respectively, and its weight and reasoning time are 7.4 M and 28 ms respectively. The experimental results show that this method can achieve the robustness and efficiency of real-time detection of orchard fruit trees.

I. INTRODUCTION

Robot has become a key aspect of the modern agricultural industry, which leverage emerging robotics, sensor, and AI technologies to automate the process of scientific data collection [1], yields estimation[2], fruit growth monitoring, and fruits harvesting[3], [4]. Among the various subsystems of an intelligent agricultural robot, navigation is an essential component that enables robot to operate autonomously in orchards [5]. It always comprises two steps: mapping and planning. The first step aims to model environments that enable robots to comprehensively understand the surroundings that they are operating in. The second step plans the motions for the robot to accomplish its tasks. An accurate and effective representation of unstructured agriculture environments is key to achieve robot autonomy in orchards.

The increasing demand for higher levels of autonomy in agricultural production places high demands on the robot's ability to understand its environment. To achieve this goal, robots need to recognise information about objects in the scene and find out their locations on the map. That is, based on the original map from the SLAM, a semantic map is created that represents the environment using a set of semantically

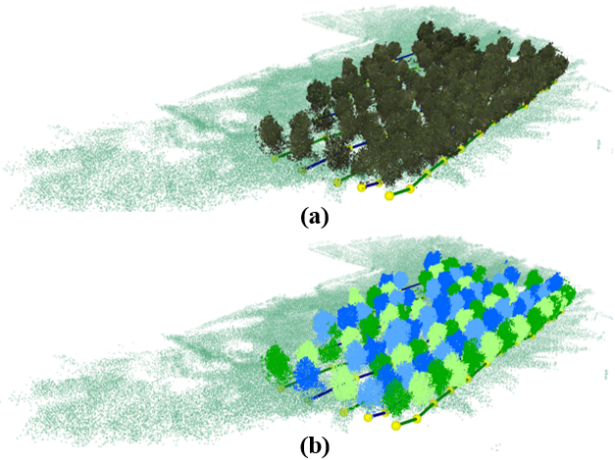


Figura 1. Demonstration of semantic map results

meaningful objects. This representation facilitates large-scale autonomy and the acquisition of actionable information in highly unstructured orchard environments because it is memory efficient, less ambiguous, and more informative. Deep learning, is an emerging and powerful tool for processing and extracting semantic information from input sensors' reading [6]. Although significant progress has been made in the construction of semantic maps using 2D image data or pseudo-3D point cloud data, semantic mapping methods directly on 3D point cloud data have not yet been widely explored. Compared with the semantic processing on 2D image data or pseudo-3D point cloud data, the semantic processing on 3D point cloud data can directly use the output of SLAM and does not require any additional calibration or data format conversion, which will lead to numerical errors and large computational consumption. However, due to the unstructured and sparse nature of 3D point clouds, how to efficiently process semantic information within point clouds remains challenging.

Simultaneous location and mapping (SLAM) technology is a basic technique that has been widely utilised in self-positioning and map construction for robotic autonomy in the field. It applies sensors such as cameras, Light Detection and Range (Lidar), radar, and IMU to acquire visual and kinetic information from their surroundings. At the front end

of the SLAM, This information will be used to compute the odometry of their motion and can be used to construct the map of the surrounding environments. At the back end of the SLAM, the map of the environments will be fine-tuned by close-loop detection and overall map optimisation. Then, an accurate landmark or point cloud map can be obtained through these procedures. Traditional SLAM focuses on extracting robust low-level geometry features to establish the right correspondence and compute the correct transient pose while lacking the ability to extract information and understand the environments that they are currently building. Therefore, traditional SLAM can only provide raw geometries that do not include any semantic information, which limits its utilisation in autonomous operations. For example, in an orchard, if the robot knows where the target fruit trees are, it can automatically find its path to the given position and finish the work, rather than having a human click on the screen each time to tell the robot specifically where to go.

In this work, by taking advantage of LiDAR-based mapping methods, a novel two-step semantic mapping framework that can achieve robotic autonomy in orchards is proposed. Firstly, we present a novel 3D detection method to accurately identify and localise objects on point cloud maps directly. Secondly, we develop a mapping framework to construct visibility graph-map for robot motion planning-. Specifically, our details contributions are as below.

- Create a fast and accurate 3D Object Detection Network (3D-ODN) to process 3D point cloud from SLAM.
- Develop a novel semantic mapping framework for orchard modelling by using information from the 3D-ODN and terrain analysis.
- Demonstrate the proposed perception and semantic mapping framework on mobile robots in orchards.

The rest of this paper is organised as follows. Section II surveys related work, followed by the proposed methodologies in Section III. Section IV-A overviews the system setup of our approach, Section III-B introduces the architecture and implementation of the 3D-TDN, Section III-C introduces the method of the semantic mapping framework. The experimental results and discussions are given in Sections IV. and then the conclusions are given in Section V.

II. RELATED WORKS

II-A. Review on Semantic SLAM

Bowman et al. put forward a kind of based on Probabilistic Data Association semantics SLAM, through the object in the image recognition to infer the categories and dimensions of the landmark and the measure information, semantic information and data correlation of sensor state and semantic landmark location problem is decomposed into discrete data correlation and landmark probability estimates, and measure the continuous optimization of state[7]. CUI et al. in the dynamic environment was proposed and visual Semantic sofslam SLAM systems: Semantic Optical FlowSLAM. SegNet semantic segmentation result to remove dynamic characteristics,

the use of static characteristics for the attitude of the camera accurately estimate, under the high dynamic scene than the ORB - SLAM2 increased by 96.73 %[8]. Chen et al. proposed the mapping method based on the surface of the extension of the use of 3 d laser range scanning, the convolutional neural network is utilized to extract semantic information filtering moving object and object classification was carried out on the laser point cloud point cloud, and pose estimation problem with the semantic constraints, build rich semantic map[9]. BAVLE et al. proposed a run on airborne robot platform of lightweight real-time visual semantic SLAM framework, the visual range of measurement and detection to the semantic object extraction combining the geometry information, enhance the robustness, build the semantic information of 3 d point cloud maps[10]. Li et al. proposed a LOAM based LiDAR assisted with the closed loop new semantic SLAM, called SA - LOAM, Using point cloud three-dimensional semantic segmentation technology for single frame radar point cloud of semantic information, this paper proposes a semantic auxiliary ICP, using semantic map the location of the mass build global consistent semantic figure in the scene[11]. Wan et al. is proposed in this paper a kind of using GPU for light indoor semantic map construction algorithm, named NGLSFusion. Optimization of lightweight network LinkNet training model, using semantic OctoMap and Voxblox fusion point cloud, reconstructing semantic graph[12]. Ouyang et al. proposed a human-in-the-loop method of semantic SLAM. Use single frame the point cloud segmentation model, the semantic information of point cloud; Finally based on point cloud semantic optimize the positioning accuracy[13]. Maps of the work above the semantic information extraction can be divided into two kinds: more than most of the semantic slam work is dividing the input image semantic network, get the meaning of the objects in the image mask, put a single frame of 3 d point cloud is mapped to the image space, get the point cloud point of semantic label. Another is the use of point cloud semantic network for single frame radar point cloud segmentation semantic segmentation, then give point cloud semantic label. Semantic map, however, the point cloud is unordered, there is no structure, the same type of semantic object is an indiscriminate point group, and no specific to the semantic information of individual objects.

II-B. Review on 3D detection

Although great success has been achieved in target detection of two-dimensional images in recent years, target detection based on three-dimensional point cloud is still an open and challenging field. Although great success has been achieved in target detection in two-dimensional images in recent years, compared with three-dimensional point clouds, two-dimensional images cannot describe the spatial distribution of objects in detail, especially in the scene where there are occlusions and overlapping objects with complex spatial distribution, there are great limitations. Target detection based on three-dimensional point clouds has begun to receive more and more attention. Tao Yu et al. proposed a mature pomegranate

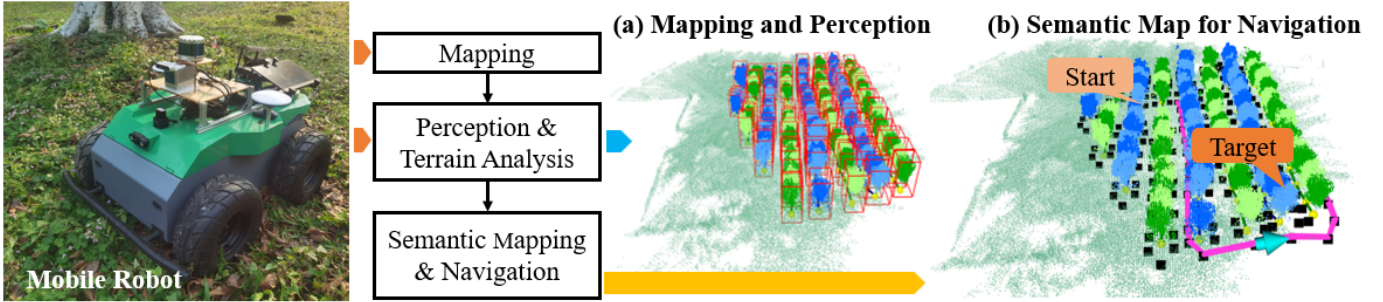


Figura 2. (a) The apple harvesting robot, (b) The attached LiDAR-D455 sensor, (c) Target-less based extrinsic calibration method and its reconstructed scene, (d) Visual sensing of the apple tree in orchard environment

fruit detection and location method based on the improved F-PointNet and 3D clustering method[14]. The method includes: (1) using RGB-D feature fusion mask R-CNN to achieve fruit detection, and using PointNet combined with OPTICS algorithm and PointFusion to segment the point cloud in the fruit cutting area. The improved F-PointNet has better performance than the classical F-PointNet, and the position error is less than 5mm. Xinxin Chen et al. proposed a pointnet-based deep learning framework, which directly processes forest point clouds, uses the voxelization strategy to subdivide the point clouds into many voxels, and uses the deep learning network to recognize the crown on the voxel scale, with the crown detection rate reaching 90 %[15]. Wei et al. proposed the point cloud segmentation network BushNet[16]. The key part of the network is the local multi-dimensional feature fusion module, which makes the network more sensitive to the shrub point cloud features; The minimum probability random sampling module samples the huge point cloud quickly and randomly; Multi-channel attention module, more accurate attention distribution, improve training efficiency. These modules have effectively improved the operation accuracy of the network, and the segmentation accuracy has been improved by 12 %.

III. METHODS

III-A. Problem statement

III-B. Perception Model

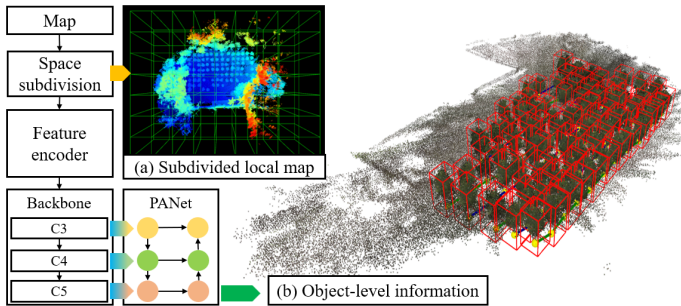


Figura 3. network architecture of tree detection

3D-ODN: A novel perception model on 3D point cloud map based on One-stage detection network is proposed. As

shown in Figure 3, the 3D-ODN model includes three steps: space subdivision, feature encoder, and detection network. 3D-ODN model accepts point cloud as inputs and estimates the bounding box of the elements in the orchards (fruit tree in our work). Firstly, the map will be subdivided into numbers of evenly-spaced and certain-sized local map. Each subdivided local map then will be feed into feature encoder. The basic idea of this step aims to extract geometry features in BEV angle and transfer the 3D point cloud map into 2D pseudo-image. Then, the 2D pseudo-images will be feed into the detection network to detect the objects. The output will be generated by combining the results from all subdivided grid.

Network Architecture: we leverage an one-stage detection network architecture to perform object-level information perception on local maps. The network utilise ResNet-50 as backbone. The input of the backbone is the encoded features of subdivided local map from the feature encoder. Then, the feature maps from C3, C4, and C5 level of the backbone are used to construct the multi-scale feature pyramid network. In this work, the Path Aggregation Network (PANet) [17] is used here to enhance the multi-scale image feature extraction and processing. Then, the processed feature maps from the PANet are used to perform detection. The combined detection results from C3, C4, and C5 level of the PANet forms the predicted objects. NMS is then used at the final to filter the prediction and generate the final results for map perception.

Feature Encoding: To leverage 2D detection network to process point cloud information, we firstly convert point cloud to a 2D pseudo image. That is, the local point cloud will be transferred to the BEV angle and be divided into the evenly-spaced grids on x-y plane. This step creates a list of pillars with ultimate extent on z-axis direction. The points within each pillars will be used to extract features of the local geometry. In this work, we utilise Viewpoint Feature Histogram (VFH) [18] and PointNet [19] to perform feature extraction, the size of each pillar is 0.5m and 0.5m in x and y directions, respectively. Some pillars is empty or only have very small number of points due to sparsity of point cloud. Therefore, we apply a requirement that only the pillars with point number large then 100 will be used to extract features. In this way, a 3D point cloud is converted into the 2D pseudo image.

Space Subdivision: To efficiently extract and process the

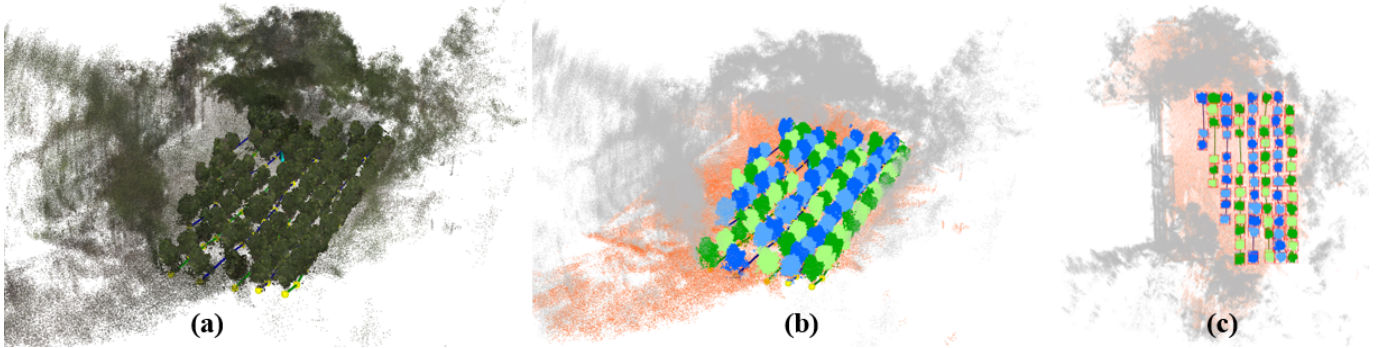


Figura 4. r3live map of orchard

geometric details in 3D geometry, a space subdivision strategy is utilised to divide a certain-sized local map from the global map (we choose 10m in this work). However, such approach encountered a implementation issue during experiments. That is, some fruit trees only have parts of its shape in local map due to space subdivision. To solve this, we proposed a sliding window detection method. After detecting a $10m \times 10m$ local point cloud map, we move the window in the positive X-axis direction by 8m in each step. This is because, based on our measurement, the maximum forward sliding distance in the radius of the fruit trees are less than 2m, so the distance of each sliding window should be ($10m$ minus the diameter of the tree crown). This sliding window approach ensures the fruit trees that are not fully covered by the last local sliding map will be fully included in the next window. The sliding window will be repeatedly moved in X-axis and Y-axis until all the areas of the global map have been traversed. Some fruit trees may have multiple predictions due to covered by multiple subdivided local maps. The Non-Maximum Suppression (NMS) is used here to find the predictions with the highest confidence and remove overlapping predictions.

III-C. Semantic Mapping

Mapping: The mapping process is performed by using by either the Lio-sam [20] or R3live [21]. For mapping using Lio-sam, the RS-Helios and external IMU (400 hz) are used. We do not use GPS in Lio-sam Mapping since the obstacles in orchards will effect the stability and accuracy of the GPS signal. For mapping by using the R3live, the livox-avia, internal IMU of livox-avia, and RGB camera are used. Both Lio-sam and R3live can perform well to modelling and describe geometry properties of the orchards. Comparably, since R3live can provide map colourisation function for visualisation. The color map of the orchard are shown in Figure 4 (a). As shown in this figure, we can see that the global map of the orchard is highly unstructured. At the mean time, points within the map are highly uneven distributed. To enable robot autonomy by using this map, the following step will respectively perform perception and terrain analysis.

Terrain Analysis: The acquired map is then processed by the perception and terrain analysis. That is, we firstly utilise

3D-ODN model to perform detection on global map. This step will generate the list of detected fruit trees. Then, a terrain analysis method based on the Cloth Simulation Filtering (CSF) algorithm [22] is utilised here to find the ground and obstacles of the orchards. The parameter of the CSF can be adjusted accordingly based on different terrain (we set $dT=0.15$ and iteration number as 100, respectively). By this way, the points of the global map are separated into traversable terrains and obstacles. By further combining the perception results of fruit trees, the points of the global map are classified into three classes: fruit trees, traversable terrains, and other obstacles, as shown in Figure 4 (b). In this figure, each tree is identified with colour that is different from their neighbour. The traversable terrains and other obstacles are colourised with the colour of red and gray, respectively. The perception and terrain analysis can be either operated online in onboard computer on real-time data stream or offline using the recorded data.

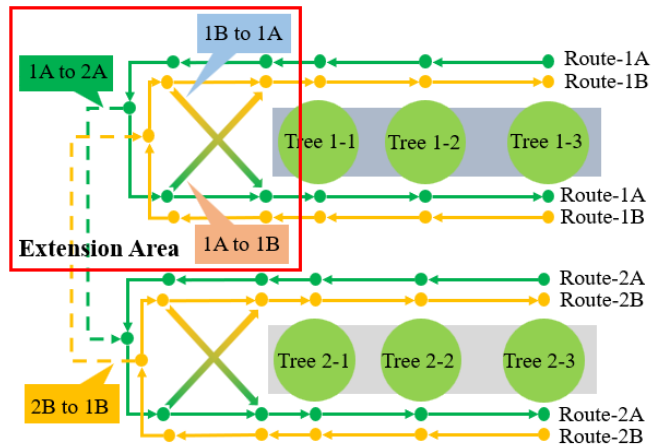


Figura 5. network architecture of tree detection

Semantic Map: The generated perception and terrain analysis results cannot be directly utilised to navigate robot in orchard. This step aims to build the navigation map for robot autonomy by giving the semantic information of orchard. Firstly, by given the position of each tree in the map, the Hough line detection algorithm is used to find the column of the tree, as shown in Figure 4 (c). The terrain between the

adjacent tree columns is the corridor that robot can transverse. Then, for each tree, we define two access point (with different forward direction) for each tree at each side of the tree column, as shown in Figure 5. The node with same direction will be connected as the loop around the tree column. For each of tree columns, there are two route with different moving direction. To allow robot change its moving direction (switch the route), robot can switch their route at the extension are of the column. Meanwhile, robot can also plan their motion from one tree column to another tree column through the connection between the route of different columns. In this way, by using the information from the semantic information, we convert the unstructured orchard environments into a structured graph map with nodes (via points) and edge (connection between via points). This step will be conducted after the finish of mapping procedure. Given the results of the perception and terrain analysis, the graph map of orchard navigation will be automatically constructed accordingly.

IV. EXPERIMENT AND DISCUSSION

IV-A. System overview

The framework of the proposed perception and semantic mapping framework is shown in Figure 2. The framework can be divided into three steps, which are mapping, perception, and semantic processing on map. Firstly, the orchard data is performed by a mobile robot with Lidar in either telecontrol or autonomous way. The mapping procedure is accomplished by using the LiDAR odometry and mapping algorithms on the acquired data. After that, the fruit trees of the orchards will be detected and localised by 3D-ODN model using the geometry information within the map. The last step, a semantic processing module that can extract terrain and topological information is developed and utilised here to construct the semantic map. Finally, the constructed semantic map will include the information of each fruit tree that can be used to plan autonomous operation and a node connection map that can navigate robot to access each fruit tree within the map.

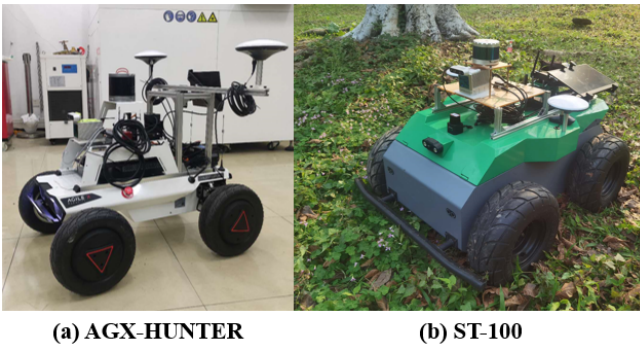


Figura 6. (a) The apple harvesting robot, (b) The attached LiDAR-D455 sensor, (c) Target-less based extrinsic calibration method and its reconstructed scene, (d) Visual sensing of the apple tree in orchard environment

Hardware and Software: The overall hardware and software configuration on our developed mobile robot to perform semantic mapping of orchards are shown in Figure 6 and

Figure 7, respectively. The sensor kit on the mobile robot (AGX Hunter-SE or ST-100 base) includes a 32-lines RoboSense Lidar (RS-Helios), a Livox-Avia Lidar, a Realsense-D435 depth camera, and an external IMU (9-axis). The data acquisition frequency of the RS-Helios, Livox-Avia, and IMU are 20Hz, 10 HZ, and 400HZ, respectively. We only acquire color image from the Realsense D435 depth camera and the data acquisition frequency is 30 HZ. The data acquired by the sensors can be used to build the initial point cloud maps of orchards by using mapping algorithm. For our case, we use Lio-sam to build the point cloud map of orchards by using the data from the RS-Helios. While for Livox-Avia Lidar, the R3-LIVE are used to build the map. The sensor kit on the robot are connected to centre computer (Nvidia Xavier) using the Robot Operating System (ROS) in Ubuntu 20.04 in Noetic version. The data transmission from the RS-Helios and Livox Avia to the centre computer are through an Ethernet port, by using rslidar-ros-driver and Livox-ros-driver, respectively. The programming of neural network model is developed based on PyTorch 1.7. The network training is performed on NVIDIA RTX-3090, while forward inference is tested on both NVIDIA RTX-3090 and NVIDIA Xavier.

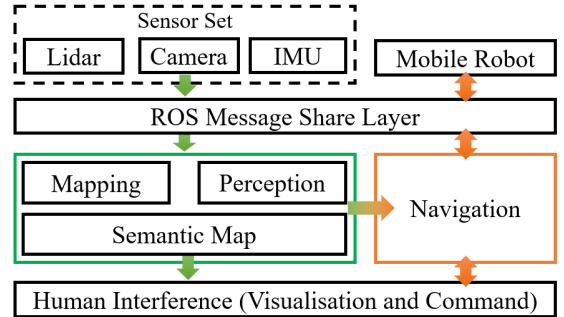


Figura 7. software architecture of system

IV-B. Data collection and Experimental methods

To achieve comprehensive lidar scanning of the orchard, we manually control the mobile robot to across each terrace in the orchard, creating a closed loop path that ends at the starting point. Using rosbag, lidar data, camera data, and IMU data were collected and input into the mapping algorithms, which generated the global point cloud map of the orchard. Data collection was conducted in the public experimental orchard in South China Agricultural University from 10:00 am to 4:00 pm, during which the distance between the tree trunks ranged from 1.2 to 2.5m, and the maximum distance from the ground to the top of the canopy was between 3.3 and 4.5m. Three orchards were included and surveyed for dataset creation. The open-source software pcd-annotation, available on Github, was used to annotate the trees in the maps by creating bounding boxes on each of trees.

In this section, we evaluated the proposed method in three experiments. First, the detection effect of different size local maps on the network is affected. Then, the influence of

different feature extraction methods on the detection efficiency and accuracy of the network is compared. Then, the mobile platform will move on the complete orchard point cloud, and the real-time detection experiment of fruit trees will be carried out. In the experiment, each network has been trained three times, and the network weight with the best verification accuracy has been saved for performance evaluation. In the experiment, mIoU, map and the detection time of the same orchard map are used-Time to evaluate the detection performance of the network. For the column header of each table below, "Tests" represents the iteration of the experiment, and "Method" represents the different combination of feature extraction method and local map size. For other column headings, we have included explanations in the corresponding text. We use 90 % of the local maps in the five orchard scenes to create the dataset for network training, and the remaining 10 % of the local maps are used for training verification and evaluation. We randomly scale the x, y, and z directions of each local point cloud map at a scale of 0-1 to enhance the data. The strengthened local map has a total of 3000.

IV-C. Ablation study of Perception

To evaluate

Evaluation on Subdivision: We first analyse the impact of different size of local maps and different resolutions on the efficiency of model operation. It should be noted that all the experiments were carried out after using the CSF algorithm to get to the ground. Table 2 shows the evaluation of network operation efficiency using local maps of different scales and different planarization resolutions on the yolo-3d model. The planarization resolution of 64, 128 and 256 are tested respectively.

Tests 1, 2 and 3 compared the impact of local maps of 5m * 5m, 10m * 10m and 15m * 15m on network performance when using density, average height and normal vector to convert into feature map at 128 * 128 resolution. The experimental results show that the different size of the local map has a greater impact on the processing time of point cloud planarization. The larger the size, the greater the number of point cloud points to be processed, and the more time it takes. The local map of 5m * 5m has the shortest running time, with an average of xxx. The map of 15m * 15m has the longest running time, with an average of xxx. However, the IOU of 10m * 10m is the highest. At the same planarization resolution, the smaller the size of the map, the smaller the area of the map represented by a single voxel, and the more pixels corresponding to the point cloud representing the fruit tree, the more obvious the fruit tree features, and the more accurate the detection. Therefore, the iou of the 10m * 10m map is higher than that of the 15m * 15m map, but the IoU of the 5m * 5m map is decreased. After the feature map is visualized, it is found that there are holes in the fruit tree after the point cloud of the fruit tree in the 5m * 5m map is converted into the feature map. When there are many holes, the IOU of the network prediction frame will be affected.

Table 1

Voxel Specification Strategy			
strategy	feature map time (s)	Predict time (s)	miou
5m*5m+64*64	0.0398	0.0168	0.809
10m*10m+64*64	0.1583	0.0168	0.798
20m*20m+64*64	0.6275	0.0168	0.772
5m*5m+128*128	0.0425	0.0268	0.725
10m*10m+128*128	0.1681	0.0268	0.812
20m*20m+128*128	0.6315	0.0268	0.796

Table 2

Feature extraction strategy			
strategy	feature map time (s)	Prediction time (s)	miou
vfh	2.13	0.0592	0.874
Proposed method	0.1681	0.0268	0.812

Tests 2, 4 and 5 compare the network performance using different planarization resolutions. The results show that the size of the planarization resolution has little effect on the feature extraction stage, but the time spent in the network prediction stage has obvious changes under different resolutions. The results show that the larger the planarization resolution is, the larger the size of the incoming network feature map is, and the more parameters are needed for network prediction, which has a direct impact on the network prediction stage. If the resolution is too high, there will be holes in the fruit tree pixels in the feature map, which will affect the accuracy of network prediction. If the resolution is too small, the detection accuracy will be reduced due to the reduction of the feature. Therefore, from the perspective of detection accuracy and detection time, it is more appropriate to select a local map of 10 m * 10 m size, and a 128 * 128 resolution feature map as the input of the network.

Evaluation on Encoder: This section uses different feature extraction strategies in network training and evaluates the detection accuracy of the obtained model. The view feature histogram (VFH) descriptor is a point cloud feature representation derived from the FPFH descriptor. The global feature extraction can be performed on the input point cloud. The calculated point cloud feature descriptor size is 308, including the components related to the view direction and the surface shape components described by the extended FPFH. The features constructed by VFH have the characteristics of scaling invariance. Test 1 of Table xxx uses VFH for feature extraction. After voxelization in the x and y directions of the local map, VFH calculation is performed on the point groups in each voxel. The 308 parameters in the calculated descriptor are stored in the pixels corresponding to the 128 * 128 size feature map of the 308 channel. Repeat this calculation until all voxels are traversed, so each local map gets a 308 * 128 * 128 feature map. Change the acceptable channel number of the convolution layer input by yolov7 to 308, and then make the prediction. In test 2, this paper uses the feature extraction method proposed in this paper. The point group in each voxel uses the average height, density, and the angle between the normal vector and the z-axis as the features, and assigns the values to the three channels respectively. After extracting the features from the local map, a 3 * 128 * 128 feature map is

generated and input into the yolov7 network for prediction. As a comparison, this paper uses pointnet++ to detect fruit tree point clouds in Test 3. Because the annotation used by pointnet++ is to label the point cloud points, it uses another manually labelled data set to label the points for training and calculates the IOU from the predicted fruit tree point cloud calculation outer rectangle box and the annotation box of the data set used for the yolov7 network.

Tests 1 and 2 show that using VFH descriptors as the point cloud feature in voxels can more explicitly express the fruit tree point cloud structure distribution in the local map than the method proposed in this paper, so that the yolo-3d network can better detect the fruit tree point cloud, and the IOU is (0.93-0.91)/0.91 higher than the method proposed in this paper. However, in terms of network efficiency in the feature extraction stage and network prediction stage, the method proposed in this paper is far better than VFH descriptor as the point cloud feature. This is because although VFH descriptors can better express the location cloud structure distribution in voxels, because each descriptor contains 308 parameters, it requires more computation than the average height, density, and normal vector angle, and 308 channels also require more computation than the three-channel feature map proposed in this paper.

Tests 3, 4 and 5 use pointnet++ to detect the fruit tree point cloud in the local map, using 1000, 2500 and 5000 sampling points respectively, and MSG as the feature extraction method. The results show that pointnet++ is the most accurate. However, because the local map is a point cloud in a space of 10 m * 10 m, although the ground point cloud is removed after using the CSF algorithm, the average number of points contained in each local map is still 10 k. Although setting a lower number of sampling points can improve the operation efficiency of pointnet++, the too low number of sampling points can not extract enough fruit tree point cloud features, resulting in a decline in the accuracy of prediction. When the number of sampling points is set to 2500 and 5000, the detection accuracy of pointnet++ is significantly improved, which is the highest among all tests, but at the same time the running time also reaches an unacceptable xxx. In summary, the method proposed in this paper can achieve a balance between recognition efficiency and accuracy. The iou of xxx and the single-frame local map detection of xxx time can meet the real-time requirements of driverless vehicles.

IV-D. Perception in Orchards

We further run lio-sam in real time with the data of xavier and 32-wire ring radar and nine-axis IMU Lio-Sam's mobile robot has tested the fruit tree detection method proposed in this paper. The Lio-sam mapping algorithm will use radar and IMU data to build the map. During the mapping process, the radar point cloud matched each time will be the registered topic will be released, and the real-time position and posture of the robot in the coordinate system with the starting point as the origin will also be updated in real time. This experiment is conducted through subscription/cloud The registered topic

obtains the orchard point cloud output by liosam for each frame. By setting the range of the orchard, the non-orchard points outside the range are removed, and the point cloud of each frame is classified into each 5 m * 5 m local map. According to the position and posture output by liosam, the 10 m * 10 m local map that the robot will enter is extracted for fruit tree point cloud detection.

The robot moves at an average speed of 1 m/s under human control. When the robot is about to reach the edge of the first line of 5 m * 5 m local map of a 10 m * 10 m local map, the two local 5 m * 5 m local maps that have been detected and are about to enter and the two local 5 m * 5 m local maps that are not detected in the forward direction will form a 10 m * 10 m local map for detection. With the robot as the center, the local map divided by 5m * 5m in the positive and negative directions of the x and y axes is known about the distribution of fruit trees. In the process of fruit tree detection while the robot is building a map, the average time for fruit tree detection on a 10m * 10m local map is 0.65s, while the maximum distance for the robot to walk at full speed is 0.65m, so the fruit tree detection within 5m meets the obstacle avoidance requirements of the robot.

IV-E. Navigation on Semantic Map

V. CONCLUSION

In this study, we propose a fast detection method of fruit tree point cloud in large-scale orchard scene based on deep learning. For Liosam, a point cloud map is reconstructed from the natural orchard using a 32-line lidar and a 9-axis IMU. It is divided into 5 m $\hat{2}$ blocks, and then four 5 m $\hat{2}$ blocks are taken to form a 10 m * 10 m local map containing a large number of points for fruit tree detection, and the position of the fruit tree in the global map is obtained in the form of a prediction frame. In the experiment, we compared the fruit tree detection efficiency of the local map at different scales and the detection performance of the network at different voxel resolutions, and found that the feature extraction of the 10 m * 10 m local map at 128 * 128 resolution can take into account the performance and efficiency of the network. The internal features of the fruit tree can be enhanced by calculating the features of the point clouds in the 8 voxels adjacent to the sample voxels. Although the feature extraction method proposed in this paper has high computational efficiency and can effectively express the feature distribution of fruit trees in the two-dimensional feature map, there is inevitably the loss of point cloud shape information. In order to know the impact of the missing information on the detection method proposed in this paper, this paper also selects VFH as the voxel point cloud feature descriptor to form a feature map for network prediction of fruit tree point clouds. At the same time, pointnet++ generated for point cloud target detection is also selected for comparison. The results show that although it lags behind the method using VFH and pointnet++ in recognition accuracy, the iou also reaches 0.88, which is of practical significance. At the same time, the method proposed in this paper can have obvious advantages in efficiency. The future research will focus on the

cooperative operation of aircraft clusters, obstacle detection, active obstacle avoidance and the integration with 5G to create unmanned agriculture with unmanned as the core. It has a good reference significance for the construction and development of China's unmanned agriculture and the reshaping of China's agricultural production model.

REFERENCIAS

- [1] H. Kang and C. Chen, "Fast implementation of real-time fruit detection in apple orchards using deep learning," *Computers and Electronics in Agriculture*, vol. 168, p. 105108, 2020.
- [2] T. Liu, H. Kang, and C. Chen, "Orb-livox: A real-time dynamic system for fruit detection and localization," *Computers and Electronics in Agriculture*, vol. 209, p. 107834, 2023.
- [3] X. Wang, H. Kang, H. Zhou, W. Au, and C. Chen, "Geometry-aware fruit grasping estimation for robotic harvesting in apple orchards," *Computers and Electronics in Agriculture*, vol. 193, p. 106716, 2022.
- [4] H. Kang, X. Wang, and C. Chen, "Accurate fruit localisation using high resolution lidar-camera fusion and instance segmentation," *Computers and Electronics in Agriculture*, vol. 203, p. 107450, 2022.
- [5] H. Zhou, X. Wang, W. Au, H. Kang, and C. Chen, "Intelligent robots for fruit harvesting: Recent developments and future challenges," *Precision Agriculture*, vol. 23, no. 5, pp. 1856–1907, 2022.
- [6] H. Kang and X. Wang, "Semantic segmentation of fruits on multi-sensor fused data in natural orchards," *Computers and Electronics in Agriculture*, vol. 204, p. 107569, 2023.
- [7] S. L. Bowman, N. Atanasov, K. Daniilidis, and G. J. Pappas, "Probabilistic data association for semantic slam," in *2017 IEEE international conference on robotics and automation (ICRA)*. IEEE, 2017, pp. 1722–1729.
- [8] L. Cui and C. Ma, "Sof-slam: A semantic visual slam for dynamic environments," *IEEE Access*, vol. PP, no. 99, pp. 1–1, 2019.
- [9] X. Chen, A. Milioto, E. Palazzolo, P. Giguerre, and C. Stachniss, "Suma++: Efficient lidar-based semantic slam," in *2019 IEEE/RSJ International Conference on Intelligent Robots and Systems (IROS)*, 2019.
- [10] H. Bavle, P. Puente, J. How, and P. Campoy, "Vps-slam: Visual planar semantic slam for aerial robotic systems," *IEEE Access*, vol. PP, no. 99, pp. 1–1, 2020.
- [11] L. Li, X. Kong, X. Zhao, W. Li, F. Wen, H. Zhang, and Y. Liu, "Sa-loam: Semantic-aided lidar slam with loop closure," 2021.
- [12] L. Wan, L. Jiang, B. Tang, Y. Li, B. Lei, and H. Liu, "Nglsfusion: Non-use gpu lightweight indoor semantic slam," *Applied Sciences*, vol. 13, no. 9, p. 5285, 2023.
- [13] Z. Ouyang, C. Zhang, and J. Cui, "Semantic slam for mobile robot with human-in-the-loop," in *Collaborative Computing: Networking, Applications and Worksharing: 18th EAI International Conference, CollaborateCom 2022, Hangzhou, China, October 15–16, 2022, Proceedings, Part II*. Springer, 2023, pp. 289–305.
- [14] T. Yu, C. Hu, Y. Xie, J. Liu, and P. Li, "Mature pomegranate fruit detection and location combining improved f-pointnet with 3d point cloud clustering in orchard," *Computers and Electronics in Agriculture*, vol. 200, p. 107233, 2022.
- [15] X. Chen, K. Jiang, Y. Zhu, X. Wang, and T. Yun, "Individual tree crown segmentation directly from uav-borne lidar data using the pointnet of deep learning," *Forests*, no. 2, 2021.
- [16] H. Wei, E. Xu, J. Zhang, Y. Meng, J. Wei, Z. Dong, and Z. Li, "Bushnet: Effective semantic segmentation of bush in large-scale point clouds," *Computers and Electronics in Agriculture*, vol. 193, p. 106653, 2022.
- [17] S. Liu, L. Qi, H. Qin, J. Shi, and J. Jia, "Path aggregation network for instance segmentation," in *Proceedings of the IEEE conference on computer vision and pattern recognition*, 2018, pp. 8759–8768.
- [18] R. B. Rusu, G. Bradski, R. Thibaux, and J. Hsu, "Fast 3d recognition and pose using the viewpoint feature histogram," in *2010 IEEE/RSJ International Conference on Intelligent Robots and Systems*. IEEE, 2010, pp. 2155–2162.
- [19] C. R. Qi, H. Su, K. Mo, and L. J. Guibas, "Pointnet: Deep learning on point sets for 3d classification and segmentation," in *Proceedings of the IEEE conference on computer vision and pattern recognition*, 2017, pp. 652–660.
- [20] T. Shan, B. Englot, D. Meyers, W. Wang, C. Ratti, and D. Rus, "Lio-sam: Tightly-coupled lidar inertial odometry via smoothing and mapping," in *2020 IEEE/RSJ international conference on intelligent robots and systems (IROS)*. IEEE, 2020, pp. 5135–5142.
- [21] J. Lin and F. Zhang, "R 3 live: A robust, real-time, rgb-colored, lidar-inertial-visual tightly-coupled state estimation and mapping package," in *2022 International Conference on Robotics and Automation (ICRA)*. IEEE, 2022, pp. 10672–10678.
- [22] W. Zhang, J. Qi, P. Wan, H. Wang, D. Xie, X. Wang, and G. Yan, "An easy-to-use airborne lidar data filtering method based on cloth simulation," *Remote sensing*, vol. 8, no. 6, p. 501, 2016.